Passivation threshold for the oxidation of liquid silicon and thermodynamical non-equilibrium in the gas phase

Mathieu Vadon [1*], Øyvind Sortland [2],
Merete Tangstad [2], Guy Chichignoud [1], Yves Delannoy [1]
*

[†1]SIMAP , [2] NTNU Department of Materials Science and Engineering
[*]Corresponding author: mathieu.vadon@simap.grenoble-inp.fr

Abstract

The present study focuses on a specific step of the metallurgical path of purification to provide solar-grade silicon: the removal of boron through the injection of H2O(g)-H2(g)-Ar(g) (cold gas process). A progressive increase of the oxidant H2O(g) concentration at injection increases the speed of the process until a silica layer appears at the surface of the liquid silicon to be purified. It then stops the purification. During the process, silica aerosols may form in the gas boundary layer. This modifies the flows of oxidants and the gas concentrations at the liquid silicon surface. This article shows with a monodimensional model that a hypothesis of thermodynamical equilibrium of silica aerosols with the gas phase in the boundary layer has to be dropped in order to explain the appearance of a silica passivating layer. The passivation threshold is defined as the limit concentration of oxidant at injection below which there is no silica on the liquid silicon surface and beyond which silica particles appear on the liquid silicon surface. Three experiments of estimation of the passivation threshold with the injection of water vapor are used to confirm an empirical criteria on the prediction of the appearance of the silica layer. Two other sets of experiments with the injection of Ar-O2 are also being studied where the kinetics of the formation of silica aerosols seems to be slower than when water vapor is used. An optimization of the speed of boron removal under the assumption of a maximal concentration of water vapor before the appearance of a passivating silica layer would require an increase of liquid silicon surface temperature from the fusion temperature of silicon.

I. Introduction

Solar grade silicon for photovoltaic cells has less purity requirements than electronic grade silicon [1]. This creates a need for the exploration of new processes which are consuming less energy than processes from the chemical route for electronic grade silicon such as the common Siemens process. Whereas the chemical route transforms the metallurgical-grade silicon (MG-Si) to be refined into gaseous species, the metallurgical route is made from a set of steps that extract the impurities from the MG-Si in its solid and liquid states.
Within the metallurgical route, solidification processes cannot remove boron efficiently due to its segregation coefficient near one. This is why other processes are needed to remove boron. One category of processes involves an impurity absorbing slag. Another category [2] involves the injection of cold gases or plasma with hydrogen and oxygen atoms, onto electromagnetically stirred and heated liquid silicon. Regarding the cold gas and plasma processes, the goal is to optimize the efficiency in the choice of the geometry, flow rate of injection, composition of the

[*]SIMAP, 1340, rue de la Piscine, 38402 Saint-Martin d'Heres, France
[†]NTNU Department of Materials Science and Engineering, Alfred Getz vei 2,7034 Trondheim, Norway

injected mixture and silicon temperature. More specifically, an increase in the concentration of H2O(g) at injection accelerates the process. However, if the concentration of H2O(g) at injection is too high, a silica passivating layer appears at the surface of the liquid silicon and stops the process. Hence, it is necessary to be able to predict the passivation threshold. The passivation threshold is the highest concentration of H2O(g) at injection at which there is no silica at the surface of the liquid silicon, and beyond which silica particles appear on the liquid silicon surface.

CFD simulations were realized with ©Ansys Fluent and have been used to model experiments from Sortland [3], in order to evaluate the mass transfer of H2O(g) towards the liquid silicon surface.

II. Thermodynamic non-equilibrium regarding silica aerosols

Homogeneization of P_{SiO}^{surf} at passivation threshold

We suppose we are at the passivation threshold in stationary conditions. The first silica particles appear under the jet where the oxidant concentration is highest. Then the stirring moves the particles from the center of the melt surface towards the crucible wall. The spreading of the particles maintains the partial pressure of SiO(g) at surface at P_{SiO}^{lim} which is the partial pressure of SiO(g) at equilibrium with Si(l) and SiO2(s/l) according to the reaction $Si(l) + SiO2(s/l) \leftrightarrows 2SiO(g)$. As illustrated in figure 1, there is adsorption of oxygen under the jet and desorption nearer to the crucible wall. Thus, the hypothesis of a global net flow of oxygen equal to zero at the surface, necessary to the hypothesis of stationary conditions, can be maintained.

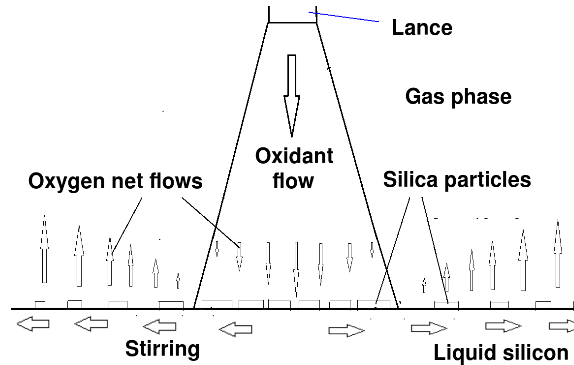

Figure 1: *Representation of adsorption and desorption flows of oxygen*

Conditions of existence of silica aerosols at the passivation threshold in stationary conditions

In this part, we are using a monodimensional model for the gas boundary layer with silica aerosols at thermodynamical equilibrium, adapting the reasoning of Vadon et al. [4] to the specific case of the passivation threshold. The main purpose of the use of a monodimensional model for a boundary layer is to prove the impossibility of a thermodynamical equilibrium over the whole boundary layer between silica aerosols and the gas at the passivation threshold. Therefore we will first make a reasoning with a zero net flow of oxygen at the liquid surface (Appendix B and C). Then we will make a similar reasoning with a positive net flow of oxygen towards the liquid

(Appendix D). Showing that both situations are not compatible with experimental observations, we will deduce that the hypothesis of thermodynamical equilibrium between silica aerosols and the gas has to be dropped.

The structure of the boundary layer in the active case (ie without silica particles on the surface) is represented in figure 2. The structure of the boundary layer in the case at passivation threshold is represented in figure 3. The corresponding model is described more in details in the appendix. In the active case, there is a homogeneous sublayer (ie without silica aerosols) near the liquid silicon at the surface, due to the reduction by the liquid silicon. However, in the passivation threshold case, if we suppose the thermodynamical equilibrium, the presence of silica particles at the surface of the liquid silicon eliminates this homogeneous sublayer.

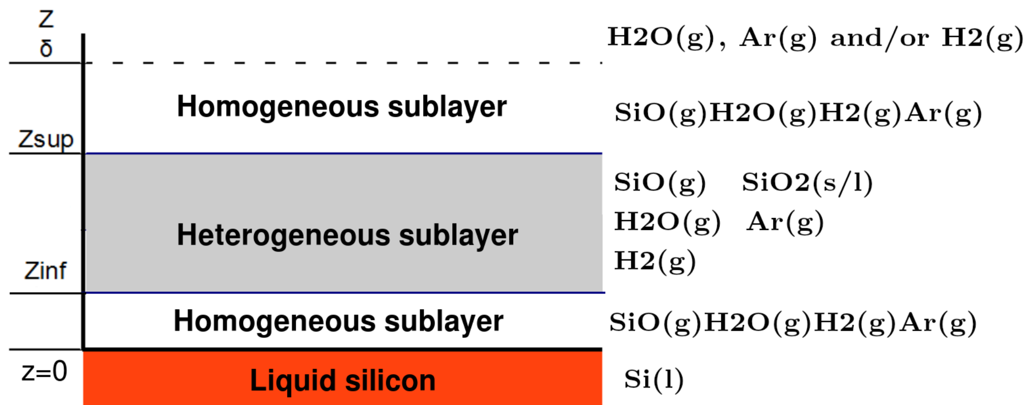

Figure 2: *Boundary layer representation in active conditions (Si(g) and SiO2(g) are also included in the model just to show that they play no significant role)*

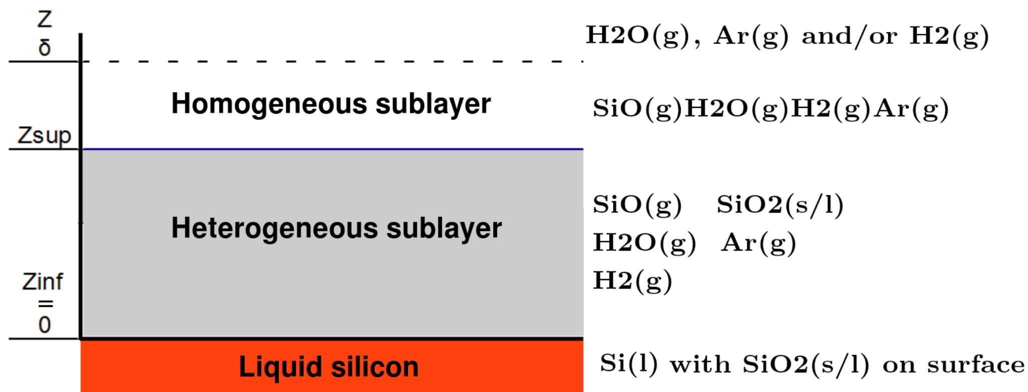

Figure 3: *Boundary layer representation at passivation threshold (Si(g) and SiO2(g) are also included in the model just to show that they play no significant role)*

Boundary layer with zero net flow of oxygen at surface

The heterogeneous sublayer (figure 3) is characterized by the presence of two phases (silica+gas) and thus has one degree of freedom less than the lower homogeneous sublayer in the case of

active conditions (figure 2). Let's consider a simplified monodimensional model in the purification conditions with only the dominant species SiO(g), H2O(g),Si(l),H2(g),SiO2(s/l). Fixing a uniform temperature in the gas phase and a net flow of zero oxygen atoms from the surface becomes equivalent to having a flow of oxidant equal to zero at the surface because there is one less degree of freedom due to the thermodynamical equilibrium that links the concentration of H2O(g) with those of SiO(g) in the presence of silica aerosols (see details at annex B). This leads to a uniform boundary layer with all concentrations equal to the concentrations at surface, which is unrealistic if we consider a boundary layer under a jet with H2O(g) and without SiO(g). Similarly, a more complex model including minority species Si(g), O2(g) and SiO2(g) as described in Vadon et al. [4] leads to unrealistically high concentrations of H2O(g) at injection to be at the passivation threshold.

If we suppose a negative temperature gradient in the non-isothermal case, this changes very little because a certain amount of SiO(g) at injection is still necessary to get into the passivation threshold, which is unrealistic (see Annex C) .

Boundary layer with non-zero net flow of oxygen at surface

In case there is a positive net flow of oxygen atoms from the gas to the liquid, the thermodynamics says this will essentially be a flow of SiO(g). The reason is that SiO(g) is a dominant species in presence of Si(l) over H2O(g), SiO2(g) and the concentrations of SiO(g) and H2O(g) are bound all over the layer by the presence of silica at thermodynamical equilibrium (see appendix D). If there is no oxygen supplied in the form of SiO(g), there will be an excess of oxygen atoms over silicon atoms that leads to the complete passivation, since silica particles on the surface are already providing oxygen atoms. We thus come to a contradiction: a gas boundary layer at thermodynamical equilibrium and passivation threshold becomes possible only in the desorption zones.

This means that in order to explain the appearance of a passivating layer in stationary conditions, we need to drop the hypothesis of thermodynamical equilibrium of silica aerosols with the gas phase .

Gap to thermodynamical equilibrium

In the appendix A, we have given an expression of the partial pressure of SiO (for active or passivation threshold conditions) at surface using a simplified model at thermodynamical equilibrium under the isothermal hypothesis (see part VII for the notations).

$$p_{SiO}^{surf,eq} = 2\left(\frac{p_{SiO2}^{s}\Psi_{H2O}p_{H2}^{eff,0}}{K_1\Psi_{SiO}\Psi_{H2}}\right)^{1/2} \tag{1}$$

Let's assume that the pressure of gaseous silica P_{SiO2}^{*} is higher than its equilibrium value by a factor α in the heterogeneous layer:

$$P_{SiO2}^{*} = \alpha P_{SiO2}^{s} \tag{2}$$

where α is assumed constant for this very first description of a non-equilibrium layer, then:

$$p_{SiO}^{surf,neq} = 2\left(\frac{p_{SiO2}^{*}\Psi_{H2O}p_{H2}^{eff,0}}{K_1\Psi_{SiO}\Psi_{H2}}\right)^{1/2} = \alpha^{1/2}p_{SiO}^{surf,eq} \propto \alpha^{1/2} \tag{3}$$

110 In case of a negative temperature gradient from the surface (cold gas process), under an
111 hypothesis of thermodynamical equilibrium, $p_{SiO}^{surf,eq}$ would be inferior to the value given at
112 equation 1, because the evolution of the equilibrium constant of the reaction of nucleation
113 $K_{nucl} = K_1/p^*_{SiO2}$ would lead to more incoming oxygen atoms precipitating into silica. But for
114 simplicity, we are going to calculate α using a value of $p_{SiO}^{surf,eq}$ calculated with an isothermal
115 hypothesis with surface temperature. This leads to an underevaluation of α in the case of a
116 negative temperature gradient.

117 At passivation threshold, the parameter α can be adjusted from p_{SiO}^{lim} (the partial pressure of
118 SiO at equilibrium with Si(l) and SiO2(s/l)) :

$$p_{SiO}^{surf,neq} = p_{SiO}^{lim} = \alpha^{1/2} p_{SiO}^{surf,eq} \tag{4}$$

119 The parameter $\alpha > 1$ describes the non-equilibrium of silica particles with the gas phase
120 and the non isothermality. $p_{SiO}^{surf,neq}$ is the experimental value of the partial pressure of SiO at
121 surface and $p_{SiO}^{surf,eq}$ is the value that the partial pressure of SiO at surface would have had, had
122 there been a thermodynamical equilibrium between the silica aerosols and the gas. It is related
123 to the speed of nucleation and growth of the particles. It depends on the speed of injection,
124 on the concentration of oxidant at injection, on the temperatures in the gas phase. The gap to
125 thermodynamical equilibrium leads to increased SiO(g) concentrations at the surface. Since the
126 densities are higher in the condensed phase, the collisions between molecules in the condensed
127 phase could be at a higher rate and the hypothesis that at the passivation threshold, there is
128 a thermodynamical equilibrium at the surface between Si(l), SiO2(s/l) and SiO(g) can still be
129 reasonably maintained. Thus, the prediction of the passivation threshold depends on the accurate
130 modeling of the nucleation and growth of silica aerosols and of the diffusion from the gas phase
131 to the growing silica aerosols.[1]

132 In order to achieve such an accurate modeling, a sufficient number of experiments of de-
133 termination of the passivation threshold are necessary; in particular experiments that test the
134 influence of the speed of injection. In the next part, we are going to present a few experiments of
135 determination of the passivation threshold to start the building of such a set of experiments.

136 III. Description of experiments to measure the passivation threshold

137 Experiments with the injection of water vapor on liquid silicon in a graphite crucible

138 In this paper, we are analyzing two sets of experiments of determination of the passivation
139 threshold.

140 The first set is taken from Sortland [3]. This is a series of injections of Ar-H2O or H2-H2O
141 gaseous mixtures on liquid silicon through a lance. The concentration of H2O(g) at injection is at
142 different levels. The highest concentration at which there is no silica observed at the surface of
143 liquid silicon and the lowest concentration at which there is silica at the surface of the liquid silicon
144 are noted. The passivation threshold is in between. The diagram of the experiments is shown at
145 figure 4, its representation in our CFD code in figure 5. The liquid silicon is electromagnetically
146 stirred.

[1] Such a complex model and the acquisition of reliable data in this regard as well as new experiments have to be done. A litterature study on the subject can be found in Vadon [5].

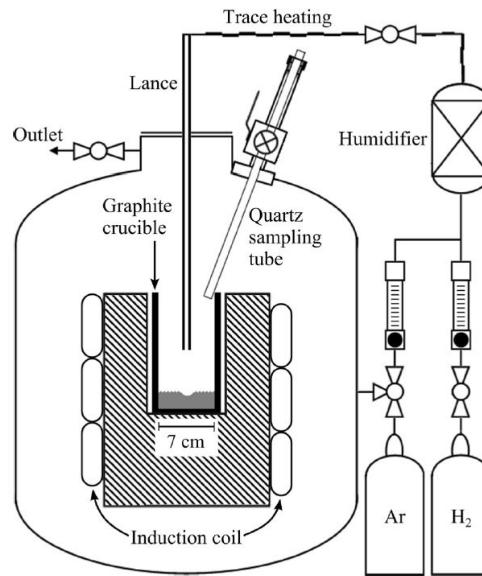

Figure 4: *Configuration of the modeled cold gas experiments. Source: Sortland [3]*

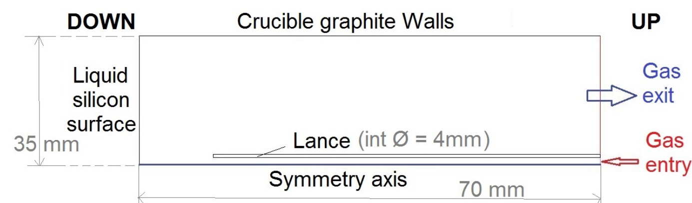

Figure 5: *Crucible representation in the CFD model*

In the series of experiments Pass_Ar and H2O_X (table 1), the injected mixture is Ar-H2O. For the experiment series, Pass_H2 it is H2-H2O.

The results for the experiments are shown in the table 2. They clearly show that an increase of surface temperature increases the passivation threshold and that the replacement of Ar by H2 makes no significant difference.

Experiments with the injection of O2 on a levitating ball

The second set of experiments is made with the injection of an Ar-O2 mixture on a levitating liquid silicon ball at an initial mass of 3.19 g. The concentration of O2(g) is increased progressively until the appearance of silica particles at the surface. A video of the ball is being filmed and the temperature and injection flows are recorded simultaneously. Due to the small mass of the ball, the surface over mass ratio is high. Thus the exothermic reaction of liquid silicon oxidation is increasing the temperature of the ball, and the increase in the concentration of O2(g) at injection leads to an increase in the temperature of the ball. Thanks to the video, we write down the temperature and O2(g) concentration at injection at the time of appearance of the first silica particules at the surface of the ball.

Between 0.026 and 0.028 Nm^3/h of injection flow of O2 (for 0.4Nm^3/h of Ar) silica is appearing at 1928 K of liquid silicon temperature. A flowmeter Brooks SLA 5850S is being used with a

maximal precision of 1% for flows in the domain 0.1 - 1 Nm^3/h. In our case, below 0.1 Nm^3/h the precision is of 0,0018 Nm^3/h which represents 6,4 % of the measured value. Given that the pressure is maintained at about 1.1 bar, there is a partial pressure of O2 at injection of about 0.070 bar. Thus, for a flow of 0,028 Nm^3/h, the relative error is 0,0018/0,028 = 6,4 % of the given value.

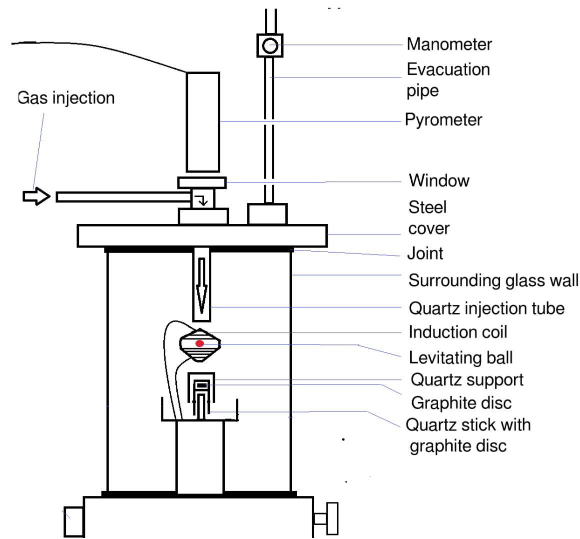

Figure 6: *Description of the device for electromagnetic levitation*

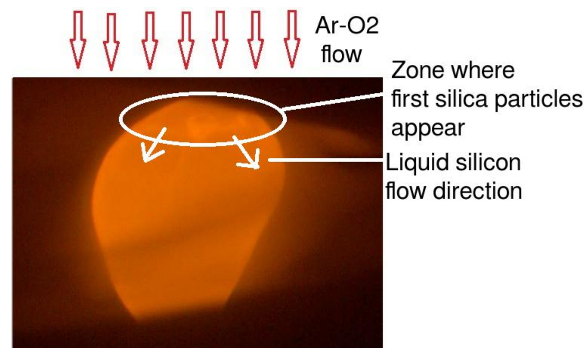

Figure 7: *Formation of silica particles at the surface of an electromagnetically levitating liquid silicon ball*

Experiments on the influence of the temperature of the liquid silicon on the passivation threshold

A set of experiments from a technical report (Saadi et al.[6]) has been done according to the geometry represented in figure 8. A mixture of Ar and O2 has been injected on liquid silicon in a graphite crucible. The concentration of O2 has been increased progressively to determine the passivation threshold and its dependence on the liquid silicon temperature. The results are represented at table 4.

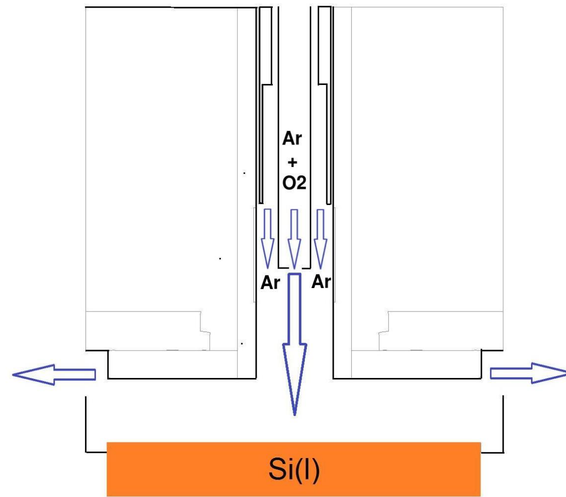

Figure 8: *Geometry for the SNC experiments*

175 # IV. Analysis of experiments

176 ## Influence of the temperature of the liquid silicon

177 Information on the influence of the temperature of the liquid silicon can be deduced from
178 the results from experiments from Sortland [3] and SNC report [6], exposed at tables 1, 2 and 4.
179 It shows a dependence on the passivation threshold that could be represented by an increasing
180 exponential function of the temperature. This is compatible with the hypothesis of a passivation
181 threshold characterized as an equilibrium between liquid silicon and surface silica particles (see
182 figure 9). This hypothesis already mentioned in Sortland [3] for experiments with the injection of
183 Ar-H2O is confirmed by new experiments with the injection of Ar-O2 from the SNC report [6].

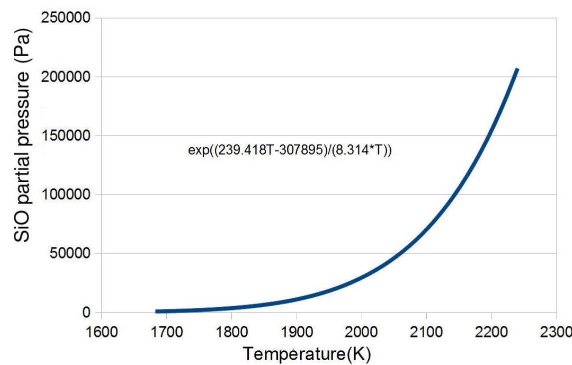

Figure 9: *SiO partial pressure at equilibrium between Si(l) and SiO2(s/l) (JANAF data [7])*

184 ## Passivation threshold with the injection of H2O(g)

In this part, we are going to check the validity of an empirical criteria from Sortland [3] for the prediction of the passivation threshold with the injection of H2O(g)-Ar(g) or H2O(g)-H2(g) on

liquid silicon. This empirical criteria is the following. Let's define the efficiency efc as the fraction of oxidant injected that reacts with Si(l) to form SiO(g). According to the empirical formula from Sortland [3], the partial pressure of H2O at the passivation threshold $P_{H2O}^{0,max}$ is given by the equation:

$$P_{H2O}^{0,max} = efc^{-1} P_{SiO}^{lim} \tag{5}$$

185 The efficiency can be measured experimentally by measuring the silicon mass loss. These
186 measurements of silicon mass loss are taken from Sortland [3] for the experiments Pass_Ar and
187 Pass_H2 . In addition to that, we have made CFD simulations with ©Ansys Fluent that predict
188 the efficiency for the H2O experiments, and for Pass_Ar and Pass_H2 as well as a verification. The
189 ability of these simulations to predict the silicon flows has been validated in Vadon et al. [10] .

190 We are using an axisymmetric stationary laminar model taking into account mass (convection,
191 diffusion) and heat transfer phenomena (convection, diffusion and radiation). The temperature
192 at the exit boundary is supposed to be 1273K but has no influence on the transport because the
193 convection is dominant for heat and mass transport at exit (see figure 5). All the same, the external
194 gas at the exit is supposed to be made of pure argon but it has no impact because the convection
195 outwards is dominant. The temperature of water vapor at injection is supposed to be 373K, but
196 the model has also little sensitivity to this parameter (Vadon[5]). The induction equations are not
197 included in the model. Instead, the zone around the melt is set as a homogeneous zone at melt
198 temperature. It is shown in Vadon [5] that due to the high speed of stirring, the mass transfer
199 inside the melt is not limiting and the temperature of the melt can be considered as homogeneous.
200 The crucible then conducts the heat with the conductivity of graphite.

201 We chose to model only the gas phase, while supposing the liquid silicon phase uniform
202 in temperature and in concentration. Regarding the cold gas experiments, Sortland [3] has
203 made experiments with the same settings except for the furnace where the frequency of the
204 electromagnetic stirring of the silicon went from 11 KHz to 4 KHz. He found identical transfer
205 coefficients at least up to an inflow of Q=2nL/mn. Regarding the experiments with the highest
206 inflow (Q16 with an inflow of Q=16 nL/mn), simulations in Sortland [3] have also shown that the
207 transport of boron in the liquid phase was probably non limiting (with a ratio of 1 to 4 between
208 the experimental transfer coefficient, and the transfer coefficient calculated by the simulation for
209 the liquid phase). Such results can be extrapolated regarding the concentrations of oxygen atoms
210 inside the melt.

211 The equations were solved by the model under ©Ansys Fluent, in stationary conditions for a
212 single phase,for 2 D axisymmetric geometries with isotropic diffusivities.

Mass conservation equation :

$$\nabla.\left(\rho\vec{v}\right) = 0 \tag{6}$$

213 Momentum conservation ($\vec{F}$ the external forces, in our case the gravity, I is the unity matrix):

$$\nabla.\left(\rho\vec{v}\vec{v}^T\right) = -\nabla p + \nabla.\left[\mu\left(\nabla\vec{v} + \nabla\vec{v}^T\right) - \frac{2}{3}\nabla.\vec{v}I\right] + \vec{F} \tag{7}$$

214 Species transport:

$$\nabla.\left(\rho\vec{v}Y_i\right) = -\nabla.\vec{J_i} + R_i \tag{8}$$

215 where R_i is the net rate of production of species i by chemical reaction, Y_i the mass fraction
216 of species i. J_i is the diffusive flow (in $kg.m^{-2}s^{-1}$), its expression is given in laminar conditions
217 and for an ideal gas at constant pressure by a component taking into account the mass fraction
218 gradients and the thermodiffusion component. The choice for the laminar model was made after
219 the comparison for the experiment with the highest speed (Q16a) had shown that the introduction
220 of the $k-\omega$ SST model made no significant difference in the results.

J_i is the solution of the equation of Maxwell Stefan (whose complex analytical solution is described in the explanatory notice) with a term that includes the thermodiffusion component:

$$\sum_{j=1,j\neq i}^{N} \frac{X_i X_j}{D_{ij}} \left(\frac{\vec{J}_j}{\rho_j} - \frac{\vec{J}_i}{\rho_i} \right) = \nabla X_i - \frac{\nabla T}{T} \sum_{j=1,j\neq i}^{N} \frac{X_i X_j}{D_{ij}} \left(\frac{D_{T,j}}{\rho_j} - \frac{D_{T,i}}{\rho_i} \right) \quad (9)$$

221 where X_i is the mole fraction, T the temperature in K, D_{ij} the binary mass diffusivity of i in j in
222 m^2s^{-1}, $D_{T,j}$ the thermal diffusion coefficient of j. The binary mass diffusivities are calculated from
223 the lennard-jones parameters and the temperature, and the thermal diffusion coefficient from the
224 molecular masses and the temperature.

225 The energy equation is given by (viscous heating is neglected in the gases):

$$\nabla. \left(\vec{v} \left(\rho E + p \right) \right) = \nabla. \left(k_{eff} \nabla T - \sum_j h_j \vec{J}_j \right) + S_h \quad (10)$$

226 where k_{eff} is the effective thermal model equal to the thermal diffusivity due to the laminar
227 model. The two terms on the right are the diffusion due to conduction and species diffusion. S_h
228 includes the volumetric heat of reaction. In the absence of volumetric reaction in the model, this
229 term is equal to zero.

230 The radiation model is a surface-to-surface model (that is the gases are transparent to radia-
231 tions), where the surfaces are represented as black bodies.

232 The integration method was using the ISAT tables, a method that stores calculated parameters
233 on different points and that calculates parameters by using previously stored parameters in points
234 with input parameters that approximate those of the point for which the calculation is being
235 performed (Ansys Manual [8] and S.B.Pope [9]).

236 We have used method B validated in Vadon et al.[10] to calculate the silicon flows. In this
237 method, only the species H2O(g), H2(g), Ar(g) are included in the model, as well as a fictive
238 species X(g), which has the thermodynamic properties of H2O(g) and the diffusivity properties of
239 H2(g). The silicon flow is calculated by estimating the flow of H2O(g) towards the surface. This
240 flow of H2O(g) towards the surface is given by the outflow of the fictive species X(g). This fictive
241 species X(g) results from the conversion of the H2O(g) molecules reaching the melt surface into
242 X(g). This flow of X(g) represents the flow of SiO(g) from the surface. This flow is divided by two
243 to take into account the nucleation and growth of silica aerosols. SiO(g) reacts entirely with H2O(g)
244 to form silica aerosols under similar conditions. Since SiO(g) comes exclusively from the oxidation
245 of Si(l) by H2O(g), it means that for one molecule of H2O(g) that reaches the liquid silicon surface,
246 one other molecule will react with SiO(g) to form silica aerosols. Apart from this, the transport
247 towards the surface of H2O(g) molecules that don't react with SiO(g) seems not to be significantly
248 modified by the reactions of formation by SiO(g) and SiO2(s/l). The diffusivity of H2(g) for X(g)
249 was chosen for reasons external to the present subject [2] and does still give an accurate description

[2]because it helps to predict accurately the concentration of H2(g) at surface which impacts the purification speed

250 of the SiO(g) flows because the evacuation of SiO(g) is non limiting for the silicon flows. As shown
251 in Vadon et al. [4] [10] the reason for this non limiting evacuation of SiO(g) is a steep decreasing
252 gradient of SiO(g) at surface due to the formation of silica aerosols at the surface with SiO(g) as
253 a reactant. The high diffusivity of H2(g) that is used for the species X(g) that represents SiO(g)
254 also helps to represent such a non limiting evacuation of SiO(g). This model supposes that the
255 dilution from surface reaction $Si(l) + H2O(g) \leftrightarrows SiO(g) + H2(g)$ and the concentration in equal
256 proportions from reaction $SiO(g) + H2O(g) \leftrightarrows SiO2(s/l) + H2(g)$ happen very near from the
257 surface. Since H2(g), a product of both reactions, has a high diffusivity, the concentration and
258 dilution compensate each other and thus have no significant influence on the transport of oxidant
259 towards the surface. We still have to divide by two the calculated flow because the H2O molecules
260 (which experimentally react with SiO(g) to form silica) in the model react with Si(l). This model
261 is well adapted for high concentrations of oxidant because it is taking both self compensating
262 phenomena of dilution and concentration into account.

263 We see in figure 10 that the empirical formula from Sortland associated with our CFD prediction
264 of the efficiency efc (equation 5) is able to predict the passivation threshold quite accurately for
265 experiments at very different temperatures. The curve of P_{SiO}^{lim} is in between the curves for active
266 and passive conditions.

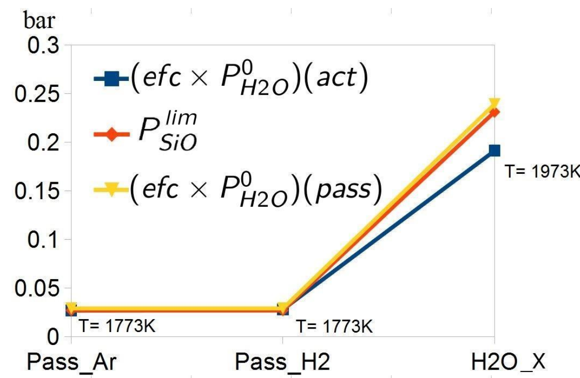

Figure 10: *For each series, Pass_Ar, Pass_H2 and H2O_X, act designates the experiment in active conditions with the highest concentration of H2O at injection and pass the experiment in passive conditions with the lowest concentration of H2O at injection.*

267 We made a numerical application for the calculation of the α factor for the case Pass_H2
268 which is easy to calculate because of the excess of H2. At 1773K, the equilibrium pressure
269 of SiO2(g) with silica is $P^s_{SiO2} = 2.85 \times 10^{-9}$ bar and $P^s_{SiO}/K_1 = 1.09 \times 10^{-6}$ bar (p^s_{SiO2}/K_1
270 being the equilibrium constant of the reaction $SiO2(s/l) + H2(g) \leftrightarrows SiO(g) + H2O(g)$) (source
271 JANAF [7]) For $P_{H2} = 1$ bar, we have at thermodynamical equilibrium of silica aerosols with
272 the gas phase: $P^{surf,eq}_{SiO} = 0.00236$ bar. Thus, using the parameters in table 5, this leads to
273 $\alpha = \left(P^{lim}_{SiO}/P^{surf,eq}_{SiO}\right)^2 = 130$. However, since we have a negative gradient from the surface, the
274 value of α is undervalued since a lower temperature favors thermodynamically the precipitation
275 of silica.

276 **Optimization of the temperature of the liquid silicon**

The purification process is at its highest speed when the concentration of H2O(g) is right at the maximum below the passivation threshold. An increase in concentration of H2O(g) causes

an increase in purification speed. This was proved experimentally (Sortland [3]). This can also be shown by reasoning on a monodimensional diffusive reactive boundary layer (equations 24 and 25 in appendix A) which shows an increase of the silicon outflow with the increase of P^0_{H2O} at injection. In Altenberend et al. [11] it was shown that regarding the purification, there is a thermodynamical equilibrium at surface between HBO(g), SiO(g),H2(g), Si(l) and B(in Si). Altenberend [11] also defined an enrichment factor as:

$$R = \frac{P^{surf}_{HBO}}{x_B P^{surf}_{SiO}} \approx \gamma_B \left(p^{surf}_{H2}\right)^{1/2} K \tag{11}$$

where K is the equilibrium constant of the reaction $B(in\ Si) + \frac{1}{2}H2(g) + SiO(g) \leftrightarrows Si(l) + HBO(g)$ and γ_B the activity coefficient of boron in liquid silicon. Then we use the approximation, verified in Vadon et al. [10] that HBO(g) and SiO(g) diffuse similarly to link the flow of boron with the flow of silicon.

$$J_B = \eta R \times x_B \times J_{Si} \tag{12}$$

Where J_B is the surface molar boron flow, J_{Si} the surface molar silicon flow and x_B the molar fraction of boron in silicon.

.

Given the decreasing evolution of the R factor with the temperature, the purification speed decrease with the temperature for a fixed concentration of H2O(g) at injection. However, it has been experimentally shown that the maximal oxidation speed before passivation increases with the temperature (table 1 combined with table 2, table 4). This poses the question of the optimal temperature.

Using the monodimensional model (see Appendix A for explanations) helps us to express the silicon flow as a function of $P^{0,max}_{H2O}$ and P^{lim}_{SiO} as in equation 13[3]:

$$J_{Si} \approx \frac{\frac{1}{2}\Psi_{H2O} p^0_{H2O} + \frac{1}{2}\Psi_{SiO} p^{surf}_{SiO}}{R\int_0^\delta \frac{T(z')}{D_{O2}(z')} dz'} \tag{13}$$

If we suppose $P^{0,max}_{H2O}$ proportional to P^{lim}_{SiO} as in the empirical formula 5 from Sortland, then $J_{Si,max}$ is proportional to $P^{lim}_{SiO} = P^{surf}_{SiO}$. Thus, under such assumption, J^{max}_B depends on temperature as does $\left(R/p^{1/2,surf}_{H2}\right) P^{lim}_{SiO}$ which is represented in figure 11 (with the removal of the dependency on p^{surf}_{H2}).

We have represented the function $\left(R/p^{1/2,surf}_{H2}\right) P^{lim}_{SiO}$ (figure 11) because the maximal rate of deboration J^{max}_B has the same evolution with the temperature as this function. We have used for this function the value recommended by Vadon et al [10] for the standard enthalpy of formation of HBO(g) ($\Delta_f(HBO(g) = -250.8 kJ/mol$) and for the activity coefficient of boron from Freis et al. [12] (equation 14). Regarding its standard molar entropy, we take the value from Gurvich [13] 202.691 kJ/mol. Other values are taken from JANAF [7].

[3]Since the molecular mass of argon (0.040kg/mol) is similar to that of SiO(g), we expect this Soret thermodiffusion effect to be not very significant. Furthermore for a negative temperature from the surface, since SiO(g) is heavier than Argon and water vapor, this thermodiffusion effect would increase J_{Si} relatively to the given formula, in a way that is an increasing function of p^{surf}_{SiO}, so this does not change the conclusions

$$log_{10}(\gamma_B^\infty) = 1105/T - 0.1105 \quad (14)$$

295 We deduce from figure 11 that an increase of temperature from the fusion temperature of
296 silicon may be advised for a maximization of the purification speed. The limit to this temperature
297 increase should then be set by the maximal acceptation of silicon mass losses during the purification
298 process.

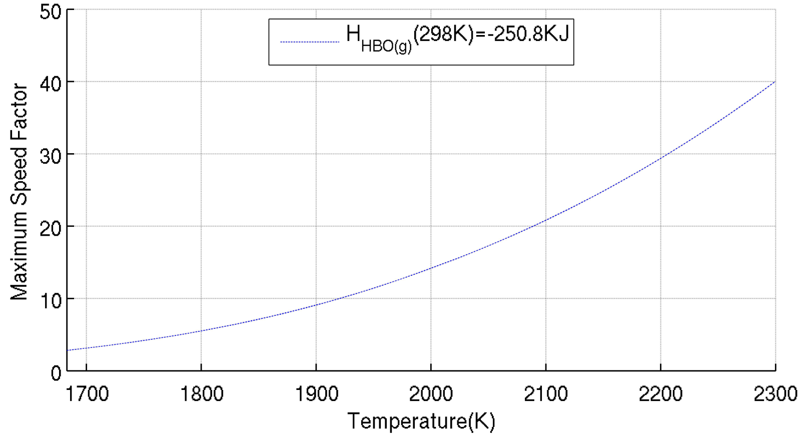

Figure 11: *Maximum speed factor Rp_{SiO}^{lim} where $p_{H2} = 1$ bar*

299 **Passivation threshold with the injection of O2(g) on levitating liquid silicon**

300 At 1928K, the partial pressure of SiO(g) at equilibrium with SiO2(s/l) and Si(l) is 0.147 bar.
301 Let's suppose that there is no influence from silica aerosols on the transport,which is compatible
302 with the experimental observations without any aerosols big enough to be observable, between
303 the jet and the levitating silicon ball.
304 Let's consider the equation for the mass transport on uniform jet on a sphere from Whitaker
305 [14] at equation 15.

$$\begin{array}{l} Sh = 2 + \left(0.4Re^{1/2} + 0.06Re^{2/3}\right) Sc^{0.4} \left(\frac{\mu_\infty}{\mu_s}\right)^{1/4} \\ 3.5 < Re < 76000 \\ 0.71 < Sc < 380 \\ Sh_X = \frac{k_X}{D_{X-Ar}/L} \\ Sc_X = \frac{\mu}{\rho D_{X-Ar}} \end{array} \quad (15)$$

306 where k_X is the transfer coefficient and L the diameter of the sphere.

307 The concentration of oxygen atoms due to the supposed absence of silica aerosols leads to the
308 equation of conservation of oxygen atoms 16:

$$\begin{array}{lcl} P_{O2}^0 & = & \frac{1}{2}\frac{D_{SiO}}{D_{O2}}\frac{Sh_{SiO}}{Sh_{O2}} \times P_{SiO}^{lim} \approx \frac{1}{2}\frac{D_{SiO}}{D_{O2}}\left(\frac{Sc_{SiO}}{Sc_{O2}}\right)^{0.4} \\ Sc_X & = & \frac{\mu}{\rho D_{X-Ar}} \\ P_{O2}^0 & = & \frac{1}{2}\left(\frac{D_{SiO}}{D_{O2}}\right)^{0.6} \times P_{SiO}^{lim} \end{array} \quad (16)$$

Using the mixing temperature $(298 + 1923) \times 0.5 = 1110K$, $\left(\frac{D_{SiO}}{D_{O2}}\right)^{0.6} \approx 0.88$ [4] , the model for a flux of O2 between 0.025Nm3/h et 0.028Nm3/h leads to a partial pressure of SiO(g) at surface between 0.138 bar and 0.153 bar in homogeneous conditions, which includes the 0.142 bar of equilibrium pressure of SiO(g) between SiO2(s) et Si(l) at the measured temperature.

On the contrary, in this case, the empirical formula of Sortland doesn't give the right range for the prediction of the passivation threshold in these conditions. We remind there is indeed a partial pressure of about 0.070 bar of O2 at injection, which means that there should be an unrealistic efficiency of about one to reach the value $\frac{1}{2}P_{SiO}^{lim} = 0.142\ bar$. It is then likely that in this case, the kinetics of nucleation and growth of silica particles was too slow to influence the transport of oxidant towards the surface of the liquid silicon. A nucleation and growth of silica that is slower under an O2(g) atmosphere than with a H2O(g) atmosphere may be an explanation for this result. However, the absence of impurities such as carbon (no crucible) and boron (non-doped electronic grade silicon) in the gas phase may also help to explain this result.

V. Conclusion and Perspectives

In the present article, we have shown that the appearance of a passivating silica layer on liquid silicon layer under a jet of O2(g) or H2O(g) with excessive oxidant concentrations can be explained only through a thermodynamical non-equilibrium of silica particles with the gas. We have verified an empirical criteria related to the prediction of the appearance of silica particles on liquid silicon with a CFD model for three experiments. However more experiments are needed as well as proper data and model for the kinetics of nucleation and growth of silica particles. An optimization of the speed of boron removal under the assumption of a maximal concentration of H2O(g) before the appearance of a passivating silica layer would require an increase of liquid silicon surface temperature. Such an increase would only be limited by the accepted losses of silicon.

VI. Acknowledgements

We thank Kader Zaidat, Benjamin Pichat, Christian Garnier and Denis Bon for their technical help for the levitation experiment. We thank the CMIRA program from Region Rhône-Alpes-Auvergne.

VII. Notations

- D_X : diffusivity of species X
- P_X partial pressure of species X
- p_X partial pressure of species X adimensionalized, from the initial pressure expressed in bar
- $\Psi_X = D_X / D_{O2}$
- J_X flow of species or atom X in $mol/m^2/s$
- k_X transfer coefficient
- $P_{O2}^{eff} = \frac{1}{2}\psi_{H2O}P_{H2O} + \frac{1}{2}\psi_{SiO}P_{SiO} + \psi_{SiO2}P_{SiO2}$ Efficient pressure for oxygen

[4] $D_{SiO} = 1.34 \times 10^{-4} m^2/s, D_{O2} = 1.65 \times 10^{-4} m^2/s$

343 • $P_{Si}^{eff} = \psi_{SiO}P_{SiO} + \psi_{SiO2}P_{SiO2}$ Efficient pressure for Si

344 • $P_{O2}^{eff,surf}$ Efficient pressure for oxygen at surface

345 • $P_{O2}^{eff,ext}$ Efficient pressure for oxygen at injection

346 • P_{Si}^{sat} saturation pressure of Si(g) which is also the pressure of Si(g) at surface

347 • P_{SiO}^{lim} partial pressure of SiO(g) at equilibrium with Si(l) and SiO2(s/l)

348 • δ thickness of the boundary layer

349 • c total molar concentration of gas

350 • x mole fraction

351 • K_{nuc} equilibrium constant of the reaction $SiO(g) + H2O(g) \leftrightarrows SiO2(s/l) + H2(g)$

352 • K_1 equilibrium constant of the reaction $SiO(g) + H2O(g) \leftrightarrows SiO2(g) + H2(g)$

353 • $Re = \frac{\rho v L}{\mu}$: Reynolds number

354 • ρ volumetric mass density

355 • L characteristic distance (diameter of the liquid silicon ball in our case)

356 • v: fluid speed

357 • μ Dynamic viscosity

358 • $Sh = \frac{k}{D_X/L}$: Sherwood number

359 • k: convective mass transfer film coefficient

360 • $Sc = \nu/D_x$: Schmidt number

361 • ν Kinematic viscosity

362 ## References

363 [1] J. Safarian, G. Tranell, and M. Tangstad: *Energy Procedia*, 2012, vol. 20, pp. 88–97.

364 [2] Y. Delannoy, M. Heuer, E. Øvrelid, and S. Pizzini: *3 Conventional and Advanced Purification*
365 *Processes of MG Silicon*, CRC press. 2017.

366 [3] Ø. S. Sortland: *Boron removal from silicon by steam and hydrogen*. PhD thesis, NTNU,Norway,
367 2015.

368 [4] M. Vadon, Y. Delannoy, and G. Chichignoud: *Metallurgical and Materials Transactions B*, 2017,
369 vol. 48, pp. 1667–1674.

370 [5] M. Vadon: *Extraction de bore par oxydation du silicium liquide pour applications photovoltaïques*.
371 PhD thesis, Université Grenoble Alpes, 2017.

372 [6] B. Saadi and G. Chichignoud:, "Projet solar nano crystal , sous lot 1.1 : Rapport intermediaire
373 contrat 2012 cnrs ferropem" tech. rep., INPG , SIMAP EPM, September 2012.

374 [7] M. W. Chase: *JANAF thermochemical tables, by Chase, MW Washington, DC: American Chemical*
375 *Society; New York: American Institute of Physics for the National Bureau of Standards, c1986.. United*
376 *States. National Bureau of Standards.*, 1986, vol. 1.

377 [8] A. Fluent: *Canonsburg, PA, USA: ANSYS Inc*, 2012.

378 [9] S. B. Pope: 1997.

379 [10] M. Vadon, Ø. Sortland, I. Nuta, C. Chatillon, M. Tansgtad, G. Chichignoud, and Y. Delannoy:
380 *Metallurgical and Materials Transactions B*, 2018, vol. 49, pp. 1288–1301.

381 [11] J. Altenberend, G. Chichignoud, and Y. Delannoy: *Metallurgical and Materials Transactions E*,
382 2017, vol. 4, pp. 41–50.

383 [12] I. Ansara, A. Dinsdale, and M. Rand: *Office for Official Publications of the European Communities*,
384 1998.

385 [13] L. V. G. I. V. V. C. B. Alcock: *Thermodynamic properties of individual substances. Vol. 3, Elements*
386 *B, Al, Ga, In, Tl, Be, Mg, Ca, Sr, Ba and their compunds, Part 1, Methods and computation*, Reading,
387 Massachusetts: Boca Raton : CRC. 1994.

388 [14] S. Whitaker: *AIChE Journal*, 1972, vol. 18, pp. 361–371.

389 [15] M. Ratto, E. Ricci, E. Arato, and P. Costa: *Metallurgical and Materials Transactions B*, 2001,
390 vol. 32, pp. 903–911.

391 [16] M. Vadon, Y. Delannoy, and G. Chichignoud:, "Prediction of the energy efficiency of an
392 ar-h2-o2 plasma torch with ansys fluent" in *8th International Conference on Electromagnetic*
393 *Processing of Materials*, 2015.

394 ## VIII. Figure captions

395 • Figure 1: Representation of adsorption and desorption flows of oxygen

396 • Figure 2: Boundary layer representation in active conditions

397 • Figure 3: Boundary layer representation at passivation threshold

398 • Figure 4: Configuration of the modeled cold gas experiments. Source: Sortland [3]

399 • Figure 5: Crucible representation in the CFD model

400 • Figure 6: Description of the device for electromagnetic levitation

401 • Figure 7: Formation of silica particles at the surface of an electromagnetically levitating
402 liquid silicon ball

403 • Figure 8: Geometry for the SNC experiments

404 • Figure 9: SiO partial pressure at equilibrium between Si(l) and SiO2(s/l) (JANAF data [7])

405 • Figure 10: For each series, Pass_Ar, Pass_H2 and H2O_X, act designate the experiment in
406 active conditions with the highest concentration of H2O at injection and pass the experiment
407 in passive conditions with the lowest concentration of H2O at injection

408 • Figure 11: Maximum speed factor Rp_{SiO}^{lim} where $p_{H2} = 1\ bar$

409

IX. Tables

Name	Total Flow (mol/s)	Pressure (bar)	Surface Temperature (K)
Pass_Ar	1.386 E-3	1.09 → 1.36	1773
Pass_H2	1.386 E-3	1.09 → 1.36	1773
H2O_X	1.386 E-3	1.36	1973

Table 1: *Parameters for the passivation experiments*

Experiment series	P_{H2O} (bar)
Pass_Ar	0.060(a)-0.065(p)
Pass_H2	0.060(a)-0.065(p)
H2O_X	0.40(a)-0.50(p)

Table 2: *Results of the passivation experiments with the highest partial pressure of H2O(g) at which there is no silica at the surface of the passivating layer (a) and the lowest partial pressure at which there is silica at the surface of the passivating layer (p)*

Generator	CELES, 50KW max, 135kHz, 500A
Pyrometer	IRCON 5R1810
Silicon	Electronic silicon "Wacker polysilicon" "N>100 Ohm/cm, P>1000 Ohm/cm", quality 6N
Window	window CF 40 in sapphire, diameter 23.8 mm
Flowmeter Ar	Brooks SLA 5850S, domain: 0-1 Nm3/H
Flowmeter O2	Brooks SLA 5850S, domain: 0-1 Nm3/H

Table 3: *Material used for the levitation experiments*

Test	Silicon Temperature (^{0}C)	Fraction O2 at passivation threshold (%)
1	1410	<3.55
2	1560	<7.06
3’	1677	>19.07
3	>1800	>19.07

Table 4: *Dependence of the passivation threshold on the liquid silicon temperature (SNC report [6])*

T=1773K
$P_{SiO}^{lim} = 0.027\ bar$
$P_{H2} = 1\ bar$
$D_{H2O} = 1.62E-3\ m^2/s$
$D_{SiO} = 1.26E-3\ m^2/s$

Table 5: *Parameters of the numerical application for the case Pass_H2 for the calculation of the α factor*

410

A. Simplified 1D Isothermal model

411 We consider a boundary layer of thickness δ, where the only reactive species out of the boundary
412 layer are H2O(g) (P^0_{H2O} at injection) and H2(g) (P^0_{H2} at injection). We remind that the convection is
413 not considered and the model included only reactive and diffusive phenomena. At the reactive
414 surface z=0, there is the liquid silicon. The structure of such a layer is given in figure 2, which
415 means there is liquid silicon at the surface.

416 Hypotheses:

417

418 • Thermodynamical equilibrium everywhere

419 • Net flow of oxygen and hydrogen atoms at surface equal to zero

420 • Sufficient dilution for the use of the Fick's Law

Let's define for this part, the effective pressures, that will be used to express the flow of oxygen and silicon atoms in a more simple way.

$$\begin{aligned} P_{Si}^{eff} &= \Psi_{Si}P_{Si} + \Psi_{SiO}P_{SiO(g)} \\ &\quad + \Psi_{SiO2}P_{SiO2(g)} \\ P_{O2}^{eff} &= \tfrac{1}{2}\Psi_{H2O}P_{H2O} + \tfrac{1}{2}\Psi_{SiO}P_{SiO(g)} \\ &\quad + \Psi_{SiO2}P_{SiO2(g)} \\ P_{H2}^{eff} &= \Psi_{H2O}P_{H2O} + \Psi_{H2}P_{H2} \end{aligned} \tag{17}$$

421 These effective pressures are defined by rearranging the partial pressures and adimensionalized
422 diffusivities Ψ in such a way that the flow of atoms of Si, H and O can be found straightfowardly.
423 The flows of atoms of Si, H and O can later be found by deriving these effective pressures via
424 Fickian-type diffusive fluxes.

425 First, let's write Fick's law for a diluted gas at uniform pressure in order to express the diffusive
426 fluxes at surface of arbitrary gas species X:

$$\begin{aligned} J_X^{mol} &= -D_X c \frac{\partial x_X}{\partial z} \\ &= -\frac{D_X}{RT}\frac{\partial P_X}{\partial z} \end{aligned} \tag{18}$$

We remind that the adimensionalized diffusivity for gas species X is written $\Psi_X = \frac{D_X}{D_{O2}}$. Thus using equation 17 and Fick's law for a diluted gas: $-\frac{2D_{O2}}{RT}\frac{\partial P_{O2}^{eff}}{\partial z}$ gives the flow of oxygen atoms:

$$-\frac{2D_{O2}}{RT}\frac{\partial P_{O2}^{eff}}{\partial z} = -D_{H2O}\frac{\partial P_{H2O}}{\partial z} - D_{SiO}\frac{\partial P_{SiO}}{\partial z} - 2D_{SiO2}\frac{\partial P_{SiO2}}{\partial z} = J_{H2O} + J_{SiO} + 2J_{SiO2} = J_O \tag{19}$$

427 Similarly, $-\frac{2D_{H2}}{RT}\frac{\partial P_{H2}^{eff}}{\partial z}$ gives the flow of hydrogen atoms and $-\frac{D_{Si}}{RT}\frac{\partial P_{Si}^{eff}}{\partial z}$ the flow of silicon atoms.
428 We have used expressions similar to Ratto et al. [15] and Vadon et al. [4]. Hence P_{O2}^{eff} and P_{H2}^{eff} are
429 used to follow flows of atoms (with a multiplicator of two) to simplify expressions further in the
430 model.

431 A reasoning on an elementary layer of thickness dz shows that $\frac{\partial^2\left(P_{O2}^{eff}-P_{Si}^{eff}\right)}{\partial z^2}=0$ because one
432 atom of silicon for every two atoms of oxygen goes from the gas phase to the silica phase, using
433 Fick's law:

$$\begin{aligned} P_{O2}^{eff}-P_{Si}^{eff} &= Az+B \\ P_{H2}^{eff} &= constant \end{aligned} \tag{20}$$

The net flow of oxygen atoms at surface is equal to zero by hypothesis, hence by Fick's law, at surface:

$$\frac{\partial P_{O2}^{eff}}{\partial z}=0 \tag{21}$$

The flow of silicon atoms at surface is given by Fick's law for diluted gases, then using equations 21 and 20 :

$$J_{Si}=-\frac{D_{O2}}{RT}\frac{\partial P_{Si}^{eff}}{\partial z}=\frac{D_{O2}}{RT}A \tag{22}$$

434 Thus, by looking at the conditions at surface (z=0) and at the top of the boundary layer ($z=\delta$)
435 the molar flow of silicon per m^2 J_{Si} can be written, using equation 20 :

$$J_{Si}=\frac{D_{O2}}{RT}\frac{\Psi_{Si}P_{Si}^{sat}+\frac{1}{2}\Psi_{H2O}P_{H2O}^{0}+\frac{1}{2}\Psi_{SiO}P_{SiO}^{surf}-\frac{1}{2}\Psi_{H2O}P_{H2O}^{surf}}{\delta} \tag{23}$$

436 Then, using thermodynamical data from JANAF [7] , we can neglect $\Psi_{Si}P_{Si}^{sat}$ and $\Psi_{H2O}P_{H2O}^{surf}$
437 compared to P_{H2O}^{0}, for P_{H2O}^{0} more than a 100Pa like in the studied cases.

$$J_{Si} \approx \frac{D_{O2}}{RT}\frac{\frac{1}{2}\Psi_{H2O}P_{H2O}^{0}+\frac{1}{2}\Psi_{SiO}P_{SiO}^{surf}}{\delta} \tag{24}$$

Let's remark that from Vadon et al. [10], there is a similar equation for non-isothermal cases, which neglects the effect of Soret thermodiffusion :

$$J_{Si} \approx \frac{\frac{1}{2}\Psi_{H2O}p_{H2O}^{0}+\frac{1}{2}\Psi_{SiO}p_{SiO}^{surf}}{R\int_0^{\delta}\frac{T(z')}{D_{O2}(z')}dz'} \tag{25}$$

SiO2(g) is a minority species ($P_{SiO2} \ll P_{SiO}$) at thermodynamical equilibrium. The gradient of P_{SiO2} doesn't play any role in the heterogeneous sublayer at thermodynamical equilibrium because its concentration is fixed by the reaction $SiO2(g) \leftrightarrows SiO2(s/l$.

$$\frac{\partial P_{SiO2}}{\partial z}=0 \tag{26}$$

438 By using the conditions at the intersection of the lower homogeneous sublayer (zero flow of
439 oxygen atoms) and the heterogeneous sublayer like in figure 2, we can thus find an analytical
440 expression of the partial pressure of SiO(g) at surface in equation 1. In the lower homogeneous

441 sublayer, the zero net flow of oxygen atoms at the surface and the absence of silica particles gives
442 with the conservation of oxygen atoms:

$$\frac{\partial P_{O2}^{eff}}{\partial z} = 0 \tag{27}$$

In the heterogeneous sublayer we have, (using K_{nucl} the equilibrium constant of the reaction $SiO(g) + H2O(g) \leftrightarrows SiO2(s/l) + H2(g)$):

$$p_{SiO} = K_{nucl}^{-1} p_{H2} / p_{H2O} \tag{28}$$

443 Therefore, at at the limit between the heterogeneous sublayer and the homogeneous sublayer
444 (the superscript "inf" is used for a variable located at this limit):

$$p_{SiO}^{inf} = K_{nucl}^{-1} p_{H2}^{inf} / p_{H2O}^{inf} \tag{29}$$

445 With a derivation of the expression of P_{O2}^{eff} in $z = z_{inf}$ at the intersection between the homoge-
446 neous sublayer and the heterogeneous sublayer, using equations 17, 28, 26 and 27:

$$0 = \frac{\partial p_{H2O}}{\partial z} \left(\Psi_{H2O} - \Psi_{SiO} K_{nucl}^{-1} p_{H2} / p_{H2O}^2 \right) + \frac{\partial p_{H2}}{\partial z} \Psi_{SiO} K_{nucl}^{-1} / p_{H2O} \tag{30}$$

Then with a simplification using the conservation of hydrogen atoms (equations 17 and 20):

$$\begin{aligned} 0 &= \tfrac{\partial p_{H2O}}{\partial z} \left(\Psi_{H2O} p_{H2O}^2 - \tfrac{\Psi_{H2O}\Psi_{SiO}}{\Psi_{H2}} K_{nucl}^{-1} p_{H2O} - \Psi_{SiO} K_{nucl}^{-1} (p_{H2}^{eff,0} - \Psi_{H2O} p_{H2O}) / \Psi_{H2} \right) \\ 0 &= \tfrac{\partial p_{H2O}}{\partial z} \left(\Psi_{H2} \Psi_{H2O} p_{H2O}^2 - \Psi_{SiO} K_{nucl}^{-1} p_{H2}^{eff,0} \right) \end{aligned} \tag{31}$$

which given the fact that the gradient of H2O is non-zero everywhere, using equation 29 for p_{SiO}^{inf}, gives the expression:

$$\begin{aligned} p_{H2O}^{inf} &= \left(\tfrac{p_{H2}^{eff,0} \Psi_{SiO}}{K_{nucl} \Psi_{H2O} \Psi_{H2}} \right)^{1/2} \\ p_{SiO}^{inf} &= \left(\tfrac{p_{H2}^{eff,0} \Psi_{H2O}}{K_{nucl} \Psi_{SiO} \Psi_{H2}} \right)^{1/2} \\ &= \tfrac{\Psi_{H2O}}{\Psi_{SiO}} p_{H2O}^{inf} \end{aligned} \tag{32}$$

Then, using the conservation of oxygen atoms in the lower homogeneous sublayer (equation 17 combined with the integration of 27 between $z = 0$ and $z = z_{inf}$) and with the thermodynamical equilibrium,since in presence of Si(l), $p_{H2O}^{surf} \ll p_{SiO}^{surf}$ and everywhere $p_{SiO2} \ll p_{SiO}$:

$$\Psi_{SiO} p_{SiO}^{surf} = \Psi_{SiO} p_{SiO}^{inf} + \Psi_{H2O} p_{H2O}^{inf} \tag{33}$$

447 hence:

$$p_{SiO}^{surf} = 2 \left(\frac{p_{H2}^{eff,0} \Psi_{H2O}}{K_{nucl} \Psi_{SiO} \Psi_{H2}} \right)^{1/2} \tag{34}$$

448 All other data can be reconstructed from known conditions at the surface and above the layer,
449 including the thickness of the lower homogeneous sublayer that is always non zero.

B. Configuration of the boundary layer at passivation threshold, isothermal case with zero oxygen atoms net flow

First of all let's remark that:

$$p_{SiO} = K_{nucl}^{-1} \frac{p_{H2}}{p_{H2O}} < K_{nucl}^{-1} \frac{p_{H2}^{eff,0}}{\Psi_{H2} p_{H2O}} \tag{35}$$

Now, let's consider the equation of net zero oxygen atom flux at surface, deriving equation 17, the difference with the previous case of non-passivation, being that this time the equation 28 of the thermodynamical equilibrium of the silica aerosols is also valid all the way down to z=0:

$$\begin{aligned} 0 &= -\frac{D_{O2}}{RT} \frac{\partial p_{H2O}}{\partial z} \left(\Psi_{H2O} - \Psi_{SiO} K_{nucl}^{-1} \frac{p_{H2}^{eff,0}}{\Psi_{H2} p_{H2O}^2} \right) \\ &= -\frac{D_{O2}}{RT} \frac{\partial p_{H2O}}{\partial z} \left(\Psi_{H2O} - \Psi_{SiO} \frac{p_{SiO}}{p_{H2O}} \frac{p_{H2}^{eff,0}}{\Psi_{H2} p_{H2}} \right) \end{aligned} \tag{36}$$

Since in the presence of Si(l) $p_{SiO}/p_{H2O} \gg 1$ and Ψ_{H2O},Ψ_{SiO} and Ψ_{H2} are of the same order, from equation 35, we deduce (P_{H2}^{eff} non infinitesimal because P_{H2O}^0 non infinitesimal):

$$\left(\Psi_{H2O} - \Psi_{SiO} \frac{p_{SiO}}{p_{H2O}} \frac{p_{H2}^{eff,0}}{\Psi_{H2} p_{H2}} \right) \simeq -\Psi_{SiO} \frac{p_{SiO}}{p_{H2O}} \frac{p_{H2}^{eff,0}}{\Psi_{H2} p_{H2}} \neq 0 \tag{37}$$

Hence $\frac{\partial p_{H2O}}{\partial z}(z=0) = 0$ and the flow is zero for all species at surface. Using the relationship 20,we deduce that the concentrations are all uniform, equal to the concentrations at surface. This is an absurdity because experimentally we have a passivation while $p_{SiO}^0 = 0$ at injection. Therefore we need to drop the hypothesis of the thermodynamical equilibrium of the silica aerosols with the gas phase at the passivation threshold in the isothermal case with zero oxygen atoms net flow.

C. Configuration of the boundary layer at passivation threshold, non-isothermal case with zero oxygen atoms net flow

We suppose we are in a case of injection of cold gases ($\frac{\partial T}{\partial z} < 0$). We suppose that the ratio of diffusivities doesn't vary with temperature, which is realistic at these high temperature (Vadon et al. [10]). This time we rewrite the equations 30 and 31, at surface:

$$0 = \frac{\partial p_{H2O}}{\partial z} \left(\Psi_{H2O} - \frac{\Psi_{SiO} K_{nucl}^{-1} p_{H2}^{eff,0}}{\Psi_{H2} p_{H2O}^2} \right) + \Psi_{SiO} \frac{\partial K_{nucl}^{-1}}{\partial T} \frac{\partial T}{\partial z} \frac{p_{H2}}{p_{H20}} \tag{38}$$

Using equation 35 and remarking again that in the presence of Si(l) $p_{SiO}/p_{H2O} \gg 1$ and Ψ_{H2O},Ψ_{SiO} and Ψ_{H2} are of the same order:

$$\frac{\partial p_{H2O}}{\partial z} \approx \frac{\partial K_{nucl}^{-1}}{\partial T} \frac{\partial T}{\partial z} \frac{p_{H2O}}{p_{SiO}} \frac{p_{H2} \Psi_{H2}}{p_{H2}^{eff,0}} \tag{39}$$

Let's now express the gradient of SiO at surface, starting from the zero flux of oxygen at surface.

$$0 = \Psi_{SiO} \frac{\partial p_{SiO}}{\partial z} + \Psi_{H2O} \frac{\partial p_{H2O}}{\partial z} \tag{40}$$

then using equation 39:

$$\frac{\partial p_{SiO}}{\partial z} = -\frac{\Psi_{H2O}}{\Psi_{SiO}} \frac{\partial K_{nucl}^{-1}}{\partial T} \frac{\partial T}{\partial z} \frac{p_{H2O}}{p_{SiO}} \frac{p_{H2}\Psi_{H2}}{p_{H2}^{eff,0}} \tag{41}$$

Since $\frac{\partial K_{nucl}^{-1}}{\partial T} > 0$ and $\frac{\partial T}{\partial z} < 0$ it means there must be $\frac{\partial p_{SiO}}{\partial z} > 0$ to be at the passivation threshold and thus an influx of silicon atoms in the form of SiO(g) which is absurd. Therefore we need to drop the hypothesis of the thermodynamical equilibrium of the silica aerosols with the gas phase at the passivation threshold in the non-isothermal case with zero oxygen atoms net flow.

We neglect the thermodiffusion effect in this demonstration, which is all the more understandable since the molecular mass of Ar (0.040kg/mol) is near from the molecular mass of SiO(g).

D. Configuration of the boundary layer at passivation threshold, isothermal case with non-zero oxygen atoms net flow

If we have a net density of flow of oxygen atoms J from the surface, we rewrite equation 31 for the flow of oxygen atoms at surface:

$$\begin{aligned} J_O &= -\frac{D_{O2}}{RT}\frac{\partial p_{H2O}}{\partial z}\left(\Psi_{H2O} - \Psi_{SiO} K_{nucl}^{-1} \frac{p_{H2}^{eff,0}}{\Psi_{H2} p_{H2O}^2}\right) \\ &= -\frac{D_{O2}}{RT}\frac{\partial p_{H2O}}{\partial z}\left(\Psi_{H2O} - \Psi_{SiO} \frac{p_{SiO}}{p_{H2O}} \frac{p_{H2}^{eff,0}}{\Psi_{H2} p_{H2}}\right) \end{aligned} \tag{42}$$

Reasoning similarly as previously, neglecting the concentration of H2O(g) at the surface to take into account the presence of Si(l):

$$J_O \approx \frac{D_{O2}}{RT}\frac{\partial p_{H2O}}{\partial z}\left(\Psi_{SiO} \frac{p_{SiO}}{p_{H2O}} \frac{p_{H2}^{eff,0}}{\Psi_{H2} p_{H2}}\right) = -\frac{D_{O2}}{RT}\Psi_{SiO}\frac{\partial p_{SiO}}{\partial z} = J_{Si} \tag{43}$$

Thus , at passivation threshold, the oxygen must be supplied in the form of SiO(g) at surface in the absorption/adsorption zones. This is absurd. Therefore we need to drop the hypothesis of the thermodynamical equilibrium of the silica aerosols with the gas phase at the passivation threshold in the non-isothermal case with a positive oxygen atoms net flow towards the liquid.